TOWARDS REPLACEMENT OF FAILED PARTS ON THE BATTLEFIELD VIA METAL CASTING IN 3D-PRINTED DESERT SAND MOLDS

Marc Pepi[a]
Jerry Thiel[b]
Nathaniel Bryant[b]
Brandon McWilliams[a]
Andelle Kudzal[a]
Jennifer Sietins[a]

[a]-Army Research Laboratory, Aberdeen Proving Ground, MD
[b]-University of Northern Iowa, Cedar Falls, IA

Abstract
The research was performed to show the feasibility and scale-up potential of production of replacement parts for long lead time DoD critical components utilizing a sand 3D-printer with indigenous desert sand to produce casting molds from a digital drawing of the actual part. Replacement and/or spare parts could then theoretically be manufactured by pouring molten metal into these molds. Success was achieved in producing parts in a laboratory setting by pouring molten aluminum into 3D-printed desert sand molds of smaller components, but scale-up proved difficult, as the fine desert sand did not fully adhere to itself, and the mold strength was less than optimal. Lessons learned could potentially be utilized to further this effort in the use of different sand, for example beach sand, which may be easier to process.

Introduction

Additive manufacturing has changed the face of conventional metal forming technologies. Conventional metal casting involves the manufacture of solid forms or patterns that sand is formed around to develop the shape of the cavity that is filled with liquid metal. The patterns or tooling for castings will often cost as much as 100 times that of the needed casting and require weeks to months to produce. The tools must then be stored, maintained and repaired between uses. Because of the amount of space required and the length of time required for producing patterns, the technology is not conducive to a mobile manufacturing platform. Additive manufacturing and digital part creation has allowed the production of castings within days rather than weeks or months. It has reduced the need for the lengthy production of costly tooling with requirements for storage space. With the proper tools and training, additive manufacturing for metal casting could allow replacement of critical cast components and provide for weapon system sustainability on or near the battlefield. This approach allows for the geometric freedom provided by 3D-printing as well as the flexibility of traditional casting [1,2]. The vision of this work was to replace the traditional sand mold equipment in the Tactical Fabrication (TACFAB) conex with a sand 3D-printer, with the hopes of using desert sand and a binder to create casting molds at the point-of-need.

Background

It would be advantageous for our warfighters to have access to technology that uses locally available indigenous materials. Several favorable outcomes of this scenario would include reduction of energy and material costs related to transportation, especially for well-established industries and support of local businesses and resource bases [3]. Shrinking the logistics tail is an important benefit of utilizing indigenous materials in-theater [4]. The 2012 Army Sustainability Report, released 31 October 2012, outlines the Army's desire to reduce the number of convoys required to resupply troops on the battlefield [5]. Reducing vulnerable convoys not only saves materiel and lives, but troops assigned to guard these convoys can actually be utilized for their intended purpose – engaging the enemy. The charter to reduce the tail in the combat zone is deemed critical to the success of the overall Army transformation, with relevance to Army future missions [6]. The Army R&D, as well as the sustainment community, should consider the reduction in the logistics footprint a principal goal. As stated in Logistics Transformation – Reducing the Logistics Footprint by Ransom et al., "Technology will be one of the primary enablers to reduce the logistic footprint, and the reduction of the logistic footprint is clearly a key element of the future battlefield" [7]. In addition, the armed forces are increasingly playing humanitarian roles in the context of assisting citizens who have lost their assets in a natural disaster and/or live in parts the world where there is no infrastructure for creating buildings, roads, bridges, or manufacture materials that can clean water, create energy, or repair machines. The ability to build and make materials with indigenous materials dually serves both the armed forces and society's needs.

State of the Technology

The intent of this program was to further 3D sand printing technology with the incorporation of a printer that utilizes CAD drawings of key components and the use of desert sand (instead of the OEM sand that is intended for use with this printer). This capability would allow the manufacture of replacement parts in-theater, which can be used as "Band-Aids" until the actual replacement parts are delivered to the forward operating bases. One-to-one replacements (where actual replacement parts would not be needed) would reduce the military logistics tail and enable point-of-need production. Work has been done in the area of using sand 3D-printers for metal casting, but none of this research has used actual desert sand. It is reported that sand is the most widely used 3D printed material over metals and plastics [8]. This prior work includes research performed by UNI through America Makes entitled "Additive Manufacturing for Metal Casting" which concluded that 3D-printing casting molds with sand made casting faster and more affordable for the automotive industry within the small and medium sized companies that make up the domestic metal casting supply chain [9]. In similar work, it was determined that binder jet sand 3D printing could be used to manufacture metal components with similar properties to those of traditional sand casting processes [10]. Comparable work has been performed at Indiana University – Purdue University Indianapolis (IUPUI) [11]. Their study concluded that a significant amount of sand could be saved by using 3D printed sand molds versus conventional sand casting. This study also concluded that the surface finish of 3D printed sand molds was higher than conventionally cast parts, and that closer dimensional tolerances could be achieved with 3D printed sand molds versus conventional sand casting. Almaghariz, et. al. claimed that 3D sand printing leads to significantly reduced lead times [12]. A lead time reduction from 10 weeks down to 12 days was provided by Connor [13] and a reduction from four months to four weeks in a case study found in Donaldson et al. [14]). Additionally, reduced labor costs (a savings of $14,000 was found by Connor [13]) as well as improved flexibility, reduced tooling and enhanced mold designs were found to be benefits from using 3D printed sand molds. When it comes to intricate designs, Singh Gill et. al. [15] concluded that 3D printed sand molds were good for parts that were thin-walled.

Approach – Proof-of-Concept with Mock Component

To determine the feasibility of using desert sand for 3D-printing casting molds, a mock component was chosen. A drawing of this mock component was converted to an .stl file by the University of Northern Iowa (UNI) and subjected to casting software which determined the optimum positioning of gates and risers needed to cast the part.

Sand Analysis / Preparation for 3D-Printing

For this program, UNI received sand from the National Training Center, Ft. Irwin, Mojave Desert, California. This sand was nicknamed "moon dust" by the Ft. Irwin staff, but the four 55-gallon drums did contain various distributions of rocks. This sand was screened by UNI to a usable US mesh size of 50 – 140 (~297 to 105µm average diameter size).

The desert sand was subjected to preliminary chemical analysis at UNI, as well as energy dispersive spectroscopy (EDS) at ARL to determine composition. Table 1 contains the results of analysis at UNI. EDS was able to detect carbon (most likely contaminant), oxygen, sodium, magnesium, aluminum and silicon. The other elements detected via chemical analysis were in too low of a quantity to be detected via EDS.

Table 1
Desert sand chemical analysis
Mass%

SiO_2	Al_2O_3	Fe_2O_3	Cr_2O_3	TiO_2	CaO	MgO	Na_2O	K_2O
91.13	4.564	0.707	0.001	0.196	1.044	0.031	1.496	0.833

UNI also calculated the pH and acid demand value (ADV) of the as-received sand, versus the same sand that had been screened to 70, 100 and 140 mesh size, respectively. As shown in Tables 2 and 3, the pH and ADV was lowered after sieving, making it more suitable for 3D-printing. Chemically, the desert sand underwent baseline testing at UNI according to AFS standard procedure. The pH test determines the basicity or acidity of the base material. This test is often associated with the ADV, or acid demand value. The ADV is used to determine how much acid is needed to cure the resin in chemically bonded sand systems. Lastly, the moisture test is conducted to determine how much water is withheld in the sand prior to experimentation. The pH was determined to be 9.57, which means the material is slightly basic. This is further supported by a high ADV of 24.5. The sand was determined to have a moisture content of 0.41%.

Table 2
pH, Acid Demand Value (ADV) and Moisture Content of
As-Received Mojave Desert Sand

pH	Acid Demand Value	Moisture
Average = 9.570	Average = 24.500	0.41

Table 3
pH and Acid Demand Value (ADV)
Screened Mojave Desert Sand

pH		Acid Demand Value	
70 mesh size	8.240	70 mesh size	10.150
100 mesh size	8.410	100 mesh size	10.200
140 mesh size	8.440	140 mesh size	9.950
Average = 8.363		Average = 10.100	

Scanning electron microscopy of the Mojave Desert sand showed a layer of dust/clay on the particles. Image J® software calculated the average diameter at 61 +/- 35µm from analysis of 50 random particles.

The commercial sand (silica) that is typically used with the ExOne® S-Max 3D-printer was compared to the indigenous sand from the Mojave Desert. Of note were differences in morphology, particle size and composition. Of these differences, particle size would not matter due to sieving that would result in particles of useful diameter for 3D-printing. Morphology may pose a problem, as particles may range from sharp and acicular to spherical in geometry, affecting packing density. Composition could also have an effect on the as-cast part, if metals such as steels were cast. For the light alloy being cast for this program (A356 aluminum), this composition would unlikely affect the physical and mechanical properties of the as-cast part.

<u>Printing of Casting Molds from Desert Sand</u>
UNI utilized the ExOne® S-Max 3D-printer to create the casting molds, which employs 8 kg of sand in two feeders. A sulfonic acid binder was mixed with the sand for 60 seconds in preparation for printing. Within the equipment, alcohol is coated onto the deposited sand/binder mixture to harden (12-minute chemical-bonded cure). The machine is capable of depositing a 0.28mm thick layer of sand in 40 seconds.

Casting molds for the mock part were made of both 3D-printed commercial sand and indigenous desert sand. The parts were subjected to micro-computed tomography (CT) inspection and stylus surface roughness measurements.

<u>Computed Tomography of Mock Components</u>
The two mock components were subjected to X-ray CT for the purpose of comparing the external surfaces and examining internal defects. A Northstar X5000 unit (with a scan power of 200kV, 1700µA and a resulting voxel size of 146.8µm) with efXCT and Volume Graphics software was utilized for this inspection. The exterior of each looked visually similar, with the part made from

the indigenous sand mold looking perhaps slightly rougher. It appeared that more internal defects were found within the actual part which was printed with indigenous sand, compared to the part made with the commercial sand, where the defects appeared to be more concentrated in the risers.

Surface Roughness of Mock Components

The surface roughness of a section from each part was measured using a Keyence laser profilometer. A sample was removed from each specimen in the same area. The average of 4 scans (2mm x 2mm) confirmed that the sample cast in commercial sand was smoother than those from the part cast in desert sand.

Metallography

Small samples of each of the mock components (made with commercial sand and with desert sand molds) were subjected to metallographic inspection. The samples were ground and polished and etched with a modified Murakami reagent. Scanning electron microscopy of the resultant structures showed that the type of sand mold used in this study had no obvious effect on microstructure.

Scale-Up – Sand Molds for an Actual USMC Amphibious Assault Vehicle (AAV) Component

Based on the success of producing a part from a mold 3D-printed with indigenous sand, scale-up to an actual weapon system component was subsequently attempted. The part chosen was a long lead-time component form a USMC AAV. The part is required to be made from casting aluminum 355 or 356 tempered to the T6 condition per QQ-A-601 (superseded by ASTM B26). It was decided that, concurrently, this component will also be additively manufactured using a 3D Systems ProX 300, using alloy Al12Si for comparison.

Desert Sand Challenges

It is understood that desert sand would most likely only be useful for low temperature alloys such as aluminum, since traditional casting uses molds comprised of granular refractory materials such as pure silica, olivine, chromite or zircon sands [16]. Reference 16 also lists other properties of traditional sand molds that could potentially be compromised by using indigenous desert sand:

- Strength enough to sustain the weight of the molten metal
- Allows for gases formed in the mold to escape
- Resistance to the erosive action of the molten metal
- Allows for unhindered metal constricting upon cooling
- Able to cleanly strip away from the cooled casting

Although a mock component was made from a mold comprised of 3D-printed indigenous sand, it turned out the sand received from Ft. Irwin, CA contained too many large pebbles and rocks, as well as a large amount of “fines”. This meant that collecting enough usable sand to make the molds for the AAV component was very difficult. The ExOne S-Max 3D-printer needs a fairly normal distribution of sand particle size from 70 to 200 mesh to operate efficiently. Methodology for sieving and screening while obtaining a usable yield provided a challenge, and it was unknown initially whether there would be enough usable sand from the amount received to make the intended casting molds. It was decided to screen the base material using a US-8 mesh riddle. This eliminated large, unusable particles from the sand. The pre-screened sand distribution was then determined by sieve analysis according to AFS-1105-00-S.

The pre-screened sand distribution was then manipulated using an automatic double-deck screener, which has three chambers that retain particular grain sizes and then exports that material into individual containers. Large particles are retained in the top chamber while fines fall through to the bottom. The sand retained in the middle chamber was collected for sieve analysis. The screener effectively eliminated coarse particles up to the US-100 mesh screen; however, it was determined by this data that there was an accumulation of fine particles in the system. It was then observed that the bottom screen was blinded by the dust present in the sand. The dust obstructed the flow of fine particles which allowed the excess fines to be retained in the middle chamber.

It was determined that the fine particles needed to be separated prior to being sent through the automatic screener, since they would be detrimental to the printing process. To accomplish this, a fluidized chamber was constructed. A fluidized chamber used air to convert granular materials from a static solid-like state to a dynamic fluid-like state. The bottom of the chamber contained air that is blown in to create pressure. The top channel contained the sand. They were separated by a porous fabric that allows air to travel through freely while still retaining the material in the top channel. An industrial blower used for a gas-fired furnace was needed to provide enough pressure for fluidization. With the equipment ready for operation, pre-screened sand was loaded into the fluidized chamber and energized. After five minutes of fluidization a sample was collected for sieve analysis.

Finalization of Sand Processing

Due to the low sand yields (approximately 35%), an additional 55-gallon drum of the Mojave Desert "Moon Dust" was forwarded to UNI. The equipment was further modified in an effort to reduce not only the larger aggregates, but also the large amount of "fines". The modified equipment was tilted to various angles to determine the optimal screening.

After receiving this fifth drum of sand, 9 barrels were fully processed to reach the finalized screen distribution described in Figure 1. There was a total yield of 884lb (401kg) of printable material as a result of the sand processing methodology from the approximately 2,500lb (1,134kg) of sand received. Since the sand distribution and processing were finalized, several baseline tests were conducted to understand the printability of the aggregate.

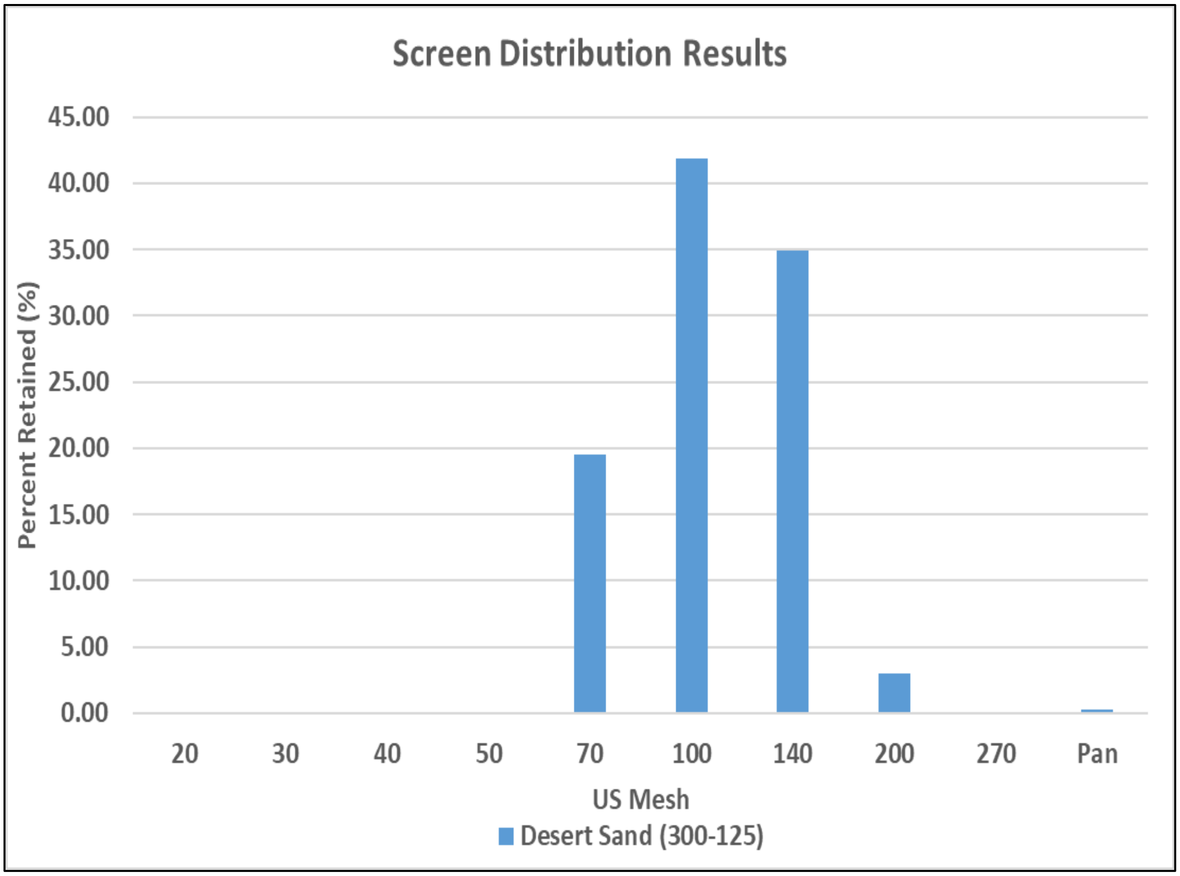

Figure 1 Accepted screen distribution of desert sand for printing.

Flowability Trials

An important consideration for sand printing is the flow characteristics of the preactivated sand. During the printing process, virgin material is siphoned into a hopper. A predetermined quantity of sand is fed into the mixing chamber where a liquid activator, toluenesulphonic acid, is introduced and the mixture is homogenized. The acid addition is calculated based on sand weight, and the printer is capable of printing in a range from 0.1 to 1% activator. When the mixer finishes a cycle, the coated sand is deposited into the recoater (the component that creates the sand layer). Several factors, including print environment humidity, activator %, and sand surface area directly influence the flow characteristics of the media. To understand the flowability of the desert sand, a granulate/powder flowability tester (powder rheometer) was used to measure how different activator levels change the sand flowability. The funnel has an interchangeable disc that is placed at the tapered end with a specific size hole placed concentrically. The hole diameters ranged from 4 to 36mm (0.16 to 1.42in).

Several common materials used for sand printing were tested alongside the desert sand for direct comparison. The sand was coated with toluenesulphonic acid at four different weight percentages (0.25%, 0.35%, 0.45% and 0.50%) and loaded into the funnel. The hatch was dropped, and if sand didn't flow out of the funnel without irritation, progressively larger hole diameters were tested until the sand did freely flow. The recorded value was the minimum hole diameter for the coated sand to flow freely. Flow was measured by starting with a small hole diameter (3mm) and loading the funnel with sand (with a specified weight percentage of activator). The hatch was dropped, and it was noted if the sand freely flowed through the hole without any irritation. If the sand did not flow, progressively larger hole diameters were tried until it did flow. For example, in Figure 2, for W730, a commercially available silica sand, the sand would flow out once the hole diameter was 20mm if it contained 0.10% TW40, but not before. After increasing the activator content to 0.25%, the sand would not freely flow out until the hole diameter was 30mm.

Figure 2 shows that the slope of the desert sand trend line was significantly lower than the other materials. This phenomena could be due to contaminants absorbing the moisture from the liquid acid. There is a much more noticeable rate of change increase in the other materials at significantly lower activator percentages. It may be worth mentioning that the other materials used are high purity silica sand and engineered ceramic materials with very low contaminants. The surface area of each sand was calculated based on the screen distribution and grain shape of the material and compared to the slope. The trend shows that higher surface area decreases the rate of sand adhesion with increasing activator content.

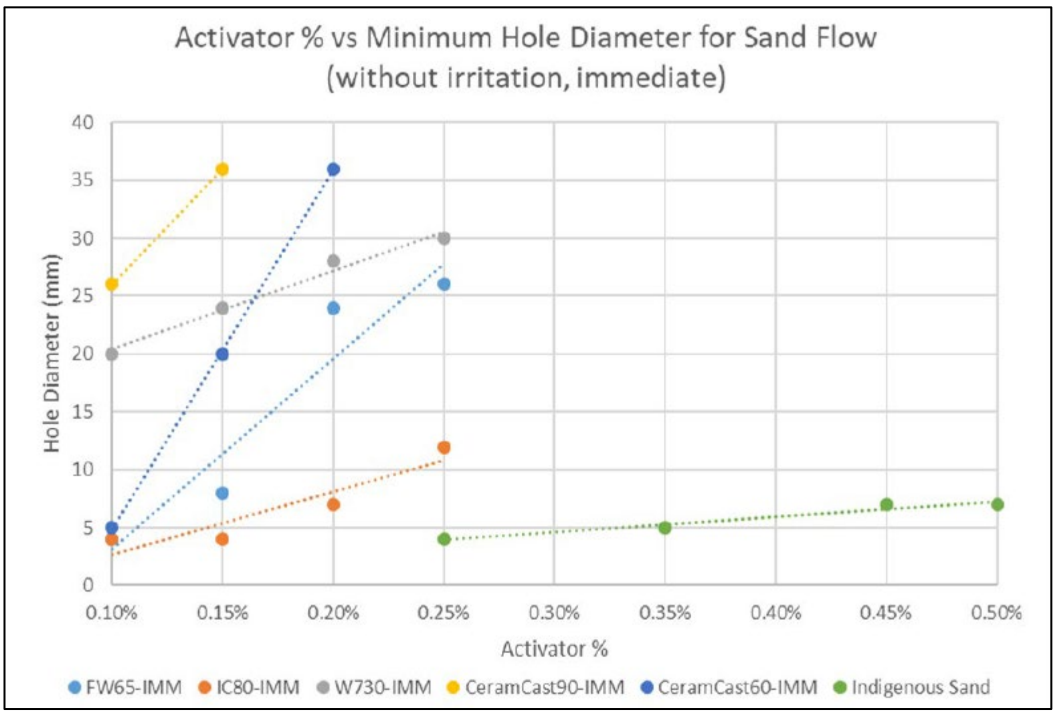

Figure 2 Flow characteristics for various sands

Another important consideration when printing sand is the acid demand value of the base sand. In acid catalyzed binder systems, such as furan, there is a quantity of acid that is needed to neutralize any basic components present in the aggregate. This gives the operator an idea of how the sand bonds. ADV trials were conducted on the desert sand to understand the bonding characteristics of the material. There were interesting results found from these experiments. When certain acids were added to the desert sand, the acid demand value increased, which is counter-intuitive. It was concluded that some sort of reaction between contaminants in the sand and the acid released more basic components into the sand; therefore, the acid demand value increased. This meant that certain acids could not be used to neutralize the aggregate. After several trials with various recipes there were no successful bonds formed with the desert sand. It also turned out that it was much harder to retain the desert sand within the recoater of the sand 3D-printer than with commercial sands

Initial Bonding Trials

As mentioned, the indigenous sand was found to have a much higher acid demand value (ADV) than the commercial sand typically used for printing (17.67 vs. 1.4 ADV, respectively). The ADV of sand is indicative of the alkalinity of the sand, and represents the chemical balances of the sand system [17]. ADV values measure the amount of milliliters of sodium hydroxide necessary to neutralize 100 grams of sand. An ADV of 17.67 indicates that 17.67 ml of NaOH are needed to neutralize 100g. The ADV has an important effect on the catalyst requirements of cold-setting acid-catalyzed binders [18]. This reference also indicates that sands with ADVs greater than 15 are not suitable for acid catalyzed binder systems, and ADVs less than 6 are preferred. Table 4 lists the many bonding trials attempted with the indigenous sand in efforts to lower the ADV. It was found that sulfuric additions were able to lower the ADV of the indigenous sand, but for the most part, none of these recipes were considered "successful". This study found that the ADV of the indigenous sand could be lowered to zero with an addition of 0.4% sulfuric acid. Bond testing was performed on the indigenous sand mixed with 0.4% sulfuric acid, 5% dry acid and 2.5% FNB resin. As shown in Table 5, the results were much lower than the nominal 80+ psi needed for casting purposes.

To increase strength, blending of the indigenous sand with commercial sand was attempted. As Table 6 shows, even with a 50-50 mix of indigenous and commercial sand, the tensile strength was still less than half of that required for printing molds.

Table 4

Initial Bonding Trials

Trial #	Resin %	Acid Catalyst %
1	1.50	0.2% toluenesulphonic acid
2	1.50	0.5% toluenesulphonic acid
3	1.50	1% toluenesulphonic acid
4	2.00	1% toluenesulphonic acid
5	1.50	1% fluoroboric acid
6	1.50	0.5% toluenesulphonic acid + 1% fluoroboric acid
7	1.50	0.325% toluenesulphonic acid + 0.175% xylenesulphonic acid 1% fluoroboric acid
8	2.00	0.65% toluenesulphonic acid + 0.175% xylenesulphonic acid
9	1.50	0.2% sulfuric acid
10	1.50	0.5% sulfuric acid
11	1.50	0.5% sulfuric acid + 1% toluenesulphonic acid
12	1.50	2% dry acid
13	1.50	4% dry acid
14	1.50	5% dry acid
15	2.00	0.2% water + 5% dry acid
16	2.00	0.2% water + 5% dry acid + 0.5% sulfuric acid

Table 5
Indigenous Sand Bonding Strength Testing

Sample #	Tensile Strength (psi)
1	11.3
2	11.2
3	5.7
4	10.2
5	10.2
6	10.6

Table 6
Blended Sand Bonding Strength Testing

Sand	TW40%	Dry Acid%	E3D%	Tensile Strength (psi) - Average
100% indigenous	0.5	5	2.5	9.9
75% indigenous / 25% FW80	0.5	2	1.5	4.5
75% indigenous / 25% FW80	0.5	3	2.0	10.8
75% indigenous / 25% FW80	0.5	5	2.5	16.4
50% indigenous / 50% FW80	0.5	5	2.5	37.3

<u>Improved Binder</u>
Due to the presence of increased fines within the screened Mojave desert sand, an improved binder was sought to deal with the higher surface area exhibited by these fines. Furan resin weight percentages that were used were already above the recommended range of the supplier to account for these increased fines. Batch mixing trials were conducted on the indigenous sand with a new, cement-based experimental binder provided by Rutgers University. Upon receipt of the material, four recipes (Table 7) were tried using a modified mixing methodology. The results were promising and tensile strengths as high as 65 psi were achieved with this new binder (Table 8). However, at such high binder concentrations, the curing occurred quickly, reducing the time that one can work with the sand mixture. Test cores (called "Gertzman" cores) were also created with these recipes and the resultant casting images are supplied within. These test cores are used to assess and evaluate metal penetration, and potential casting-related defects on a test scale, without making full-scale castings. A surface plate casting was also created to measure the surface roughness of metal cast against the indigenous material. It was found that it behaved most similarly to a commercial, 44 AFS-GFN silica sand.

<u>Testing Methodology</u>
Small Batch Mixing - A representative, 3500g batch of pre-screened indigenous sand was placed in a small batch mixing container. The first part of the experimental binder system, the "N-400" powder, was then introduced at the specified weight percentage defined by the recipes in Table 7. The result was mixed for 3 minutes, but the sand/powder mixture was flipped every 1.5 minutes. Next, either the specified weight of "X2" or "X11" binder was added and mixed for 1 minute.

This sand was used to create standard tensile specimens, Gertzman test cores, and a surface plate test core.

Melting Operations

The Gertzman test molds were cast using class 30 gray iron, with a pouring temperature of 1440°C (2625°F). After 24 hours, shakeout occurred, and the resultant castings were sectioned and the evaluation areas were imaged using a high-resolution camera. Comparisons were drawn between both sand type and the presence of a graphite-based refractory mold wash. A surface plate mold made from desert sand utilizing recipe 4 was also cast using A356 aluminum to measure the metal surface roughness. Using a Taylor-Hobson stylus profilometer, eight measurements were gathered on the resultant casting and the results were compared to data from a previous investigation [19].

Tensile Testing

Table 7 also lists the tensile strength results from the small batch mixing recipes. The first attempt, recipe 1, did not achieve any strength; however, upon increasing the overall addition rates of both the N-400 powder and X2 liquid material strengths of approximately 12.5 psi were achieved after 24 hours (the typical strength development period for foundry binders). Recipes 3 and 4 utilized the X11 liquid material rather than the X2, and the addition rates were increased. It can be observed that 24 hour strengths of approximately 65 psi were obtained using the last recipe, but it was noted that the work and strip time of the material was quite fast (as low as 3 minutes), and any addition rates higher than those tried in this recipe would cure too quickly. X11 exhibited a much faster curing rate than X2, so higher addition rates may be tried utilizing X2 to potentially achieve higher maximum strengths. Rutgers mentioned that the X11 would have higher strength than the X2, based on the chemistry.

Table 7

24-hour tensile strength results from each small batch mixing trial conducted

Recipe ID	Composition (wt% BOS)	24Hr Tensile Strength (psi)
Recipe #1	4% N-400, 5% X2, Desert Sand	0.0
Recipe #2	6% N-400, 7.5% X2, Desert Sand	12.5
Recipe #3	6.2% N-400, 7.5% X11, Desert Sand	28.7
Recipe #4	9% N-400, 10.9% X11, Desert Sand	64.9

Gertzman Casting Results

The Gertzman casting result for a commercial, 57 GFN silica sand utilizing 4% N-400 powder and 5% X2 binder without the application of the graphite-based refractory coating showed metal penetration defects in the evaluation area. This is typical for baseline silica sand and were effectively eliminated when the graphite-based refractory coating was applied.

The first Gertzman casting result for the indigenous sand was created using 6% N-400 and 7.5% X2 binder. This core was cast without any refractory mold coating, and as a result, there was severe metal penetration in the evaluation area. Large particles could be seen adhering to the casting surface, which were irremovable by sand blasting at 80psi. When the graphite-based refractory mold wash was used with the indigenous sand, the overall penetration was reduced but there were still a significant number of defects present, including embedded large particles on the evaluation surface.

Surface Roughness Results

Table 8 presents the results from the surface roughness measurements. The desert sand yielded an average surface roughness of 282.5 RMS, or root mean squared. When comparing this number to data gathered for silica sand during a prior investigation [19], it was most similar to a commercial, 44 GFN material.

Table 8

Surface roughness results measured from indigenous sand casting.

Measurement #	Result (RMS - μin)
1	300 (273 Ra – converted)
2	280 (255 Ra – converted)
3	240 (218 Ra – converted)
4	240 (218 Ra – converted)
5	310 (282 Ra – converted)
6	320 (291 Ra – converted)
7	340 (309 Ra – converted)
8	230 (209 Ra – converted)
Average	*282.5* (257 Ra – converted)

Process Simulation

Magmasoft® software was utilized to simulate the pouring and solidification of the AAV component made from A356 aluminum alloy. This software is commonly used to reduce/eliminate the porosity, shrinkage and other deleterious casting defects, and suggests optimal location of gates, risers and chills. Initial software results of casting the AAV component was optimized with strategically placed gates and risers, which pushed potential defects out of the actual component.

Mold from Indigenous Sand with Improved Binder

An attempt was made to pack indigenous sand (with the improved binder) into molds 3D-printed with the IC80 commercial sand (silica). Unfortunately, even with the new binder, the strength was not sufficient, and the indigenous sand mold broke upon removal.

3D-Printing Casting Mold from Commercial Sand

As a proof-of-concept, cope and drag patterns were 3D-printed with commercial sand based on the optimized results of the Magmasoft® software. IC80 commercial sand was utilized for these pieces. This was 3D-printed from the IC80 commercial sand that was coated with polyurethane. The resultant part is shown in Figure 3.

Recommended Post-Processing

As mentioned previously, the USMC AAV component is required to be fabricated from 355 or 356 aluminum casting alloy and tempered to the T6 temper condition, meaning an additional heat treatment would be needed for any AAV parts made from molds 3D-printed from indigenous sand. The T6 temper consists of solution heating following by an artificial age. The artificial age (referred to as precipitation heat treatment) is a lengthy, low-temperature process where temperature control/uniformity is critical [20]. The required heat treatments for these alloys are listed in Table 9, as found in the governing specification (ASTM B917 [21]).

Figure 3 Cast A356 AAV part from 3D-printed molds using commercial sand.

Table 9

Required Heat Treatments for Aluminum Casting Alloys 355 and 356 [21]

Alloy	Solution Heat Treatment [1,2]		Precipitation Heat Treatment [3] (Temper = T6)	
	Metal Temperature +/- 12°C (10°F)	Time at Temperature (h)	Metal Temperature +/-12°C (10°F)	Time at Temperature (h)
355	527 (980)	6 to 12	154 (310)	3 to 5
356	538 (1000)	6 to 12[4]	154 (310)	3 to 5

1 – Quench in water at 66 to 100°C (150 to 212°F).
2 – Time at solution temperature may be increased for section thickness over 1 in.
3 – No quenching required. Cool in still air outside the furnace.
4 - Solution time may be reduced when the silicon eutectic has been well modified such as when modified with Sr or Na.

AM Builds of Component Using Aluminum Alloy

The intent of this project was to compare properties of an AAV part cast in a mold made from indigenous sand to those of a part built with metal additive manufacturing. The following outlines the work performed in building this component with aluminum powder via additive manufacturing.

Aluminum Powder - ARL also AM built three AAV parts with the 3D Systems ProX 300 3D-printer, using manufacturer recommended Phenix PS2585-18 casting aluminum alloy AlSi12 powder, the chemical analysis of which is listed in Table 10. The powder was found to be free flowing with a tap density of 43.3%. Tap density is the packing density of the powder without any additional applied pressure/compaction and is the mass divided by the final volume of the powder which is normalized by the theoretical density of 2.6 g/cc.

Table 10

Chemical analysis of AlSi12 powder used for AM build [22]

Element	Result (wt %)
Carbon	0.003
Sulfur	<0.001
Oxygen	0.178
Nitrogen	<0.001
Iron	0.22
Silicon	12.0
Manganese	0.020
Chromium	0.016
Gallium	0.013
Nickel	0.021
Lead	0.028
Tin	0.013
Titanium	0.036
Zinc	0.063
Aluminum	remainder

Notes: No other elements detected in excess of 0.01% wt %

Methods: carbon & sulfur: combustion infrared detection per ASTM E1019-11
hydrogen: inert gas fusion per ASTM E1447-09
oxygen & nitrogen: inert gas fusion per ASTM E1019-11
all others: direct current plasma emission spectroscopy per ASTM E1097-12

Scanning electron microscopy of the AlSi12 powder was performed on a Hitachi S4700 Field Emission SEM. Figure 4 shows the powder at 500x magnification. For the most part, the powder was spherical, with a mix of oblong particles.

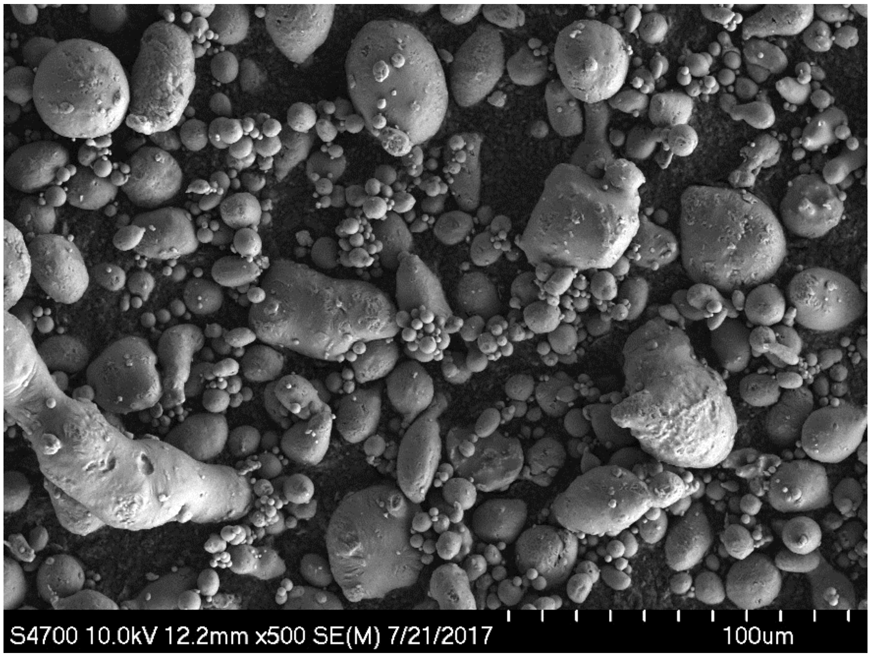

Figure 4 SEM of the 3D Systems AlSi12 powder at 500x magnification.

Additive Manufacturing Build - The printer utilized was the 3D Systems ProX300®. The height of this part was close to the limit that this machine can build, and was the tallest build by ARL on this equipment, up to this point. After pre-processing, the parts were completed after 100-hours (machine time) of build time. A total of 5,000 40μm layers were utilized to complete these parts. Although exterior supports were used, there were no internal supports associated with this build.

The processing parameters used to build these parts are listed in Table 11. The parameters are listed not only for the actual parts, but for the structure that supported the part during the build. The part is shown in Figure 5 after removal from the build plate, and support material.

Table 11
Processing parameters used for AM builds

Parameter	Build	Support
Laser power (%)	45	80
Laser power (W)	225	400
Laser speed (mm/s)	1200	2500
Layer thickness (μm)	40	40
Hatch spacing (μm)	70	70
Interlayer rotation angle (deg)	45	45
Hexagon radius (μm)	5000	25000
Hexagon overlap (μm)	100	100

Part Characterization

Dimensional Verification - The AM parts were measured in a metrology laboratory located at the Army Research Laboratory to determine conformance to the governing 2-dimensional drawing. There were some glaring discrepancies noted on the first three AM-built parts. The wall thickness of the part went from 0.792cm (0.312-inch) to 0.254cm (0.1-inch) when converting to a .stl file. Additionally, the inner diameter was out of tolerance and there was some overlap on one of the lips. Sagging of one of the corners was also noted, most likely due to the weight of the build. Finally, one of the bolt through-holes was out-of-round and the centerline distance between the bolt holes was 6.6cm (2.6-inch), instead of the required 6.7 cm (2.65-inch). The .stl file was amended and an AM build (two per plate) was accomplished. One of these parts was also subjected to dimensional verification which showed conformance to all dimensions.

Figure 5 AM-built part using amended .stl file ensuring proper dimensions.

Computed Tomography of AM Built AAV Component - The AM parts were subjected to X-ray computed tomography (CT) in order to inspect for internal defects. A Northstar X5000 unit (with a scanning power of 180kV and 140µA and a voxel size of 129.5 µm) with efXCT, CTVox, and CTAn software was utilized for this inspection. Evidence of witness lines can be seen on the outer diameter which was caused by a pause in the build due to a power outage. The lines were horizontal to the build direction. CT inspection for porosity both within the support material and the as-built material determined that the support material exhibited a porosity of 0.48% while the as-built part had 0.59% porosity.

CT inspection was also used to determine defect sphericity for both the support and as-built material. Sphericity is a measure of porosity shape, as this defect is formed by trapped gas bubbles, and is generally round in morphology. It was found that there was not a strong change in the sphericity with the change in processing parameters. In addition, it was noted that support and build defect volumes were comparable for defects below 10,000 μm^3, but slightly larger defects were found in the as-built parts.

Density Measurements - The density of the AM built parts (using tensile specimens) was determined with the Archimedes method:

$$\rho = \frac{(m_{dry} * \rho_{water})}{(m_{dry} - m_{wet})}$$

Table 12 contains the results of this analysis. No appreciable density difference was noted between the as-built specimens which were also similar to the supports. These results compared favorably with the 2.66 g/cc theoretical bulk density reported in literature [23].

Table 12
Density Measurements for As-Built AlSi12 Powder

$AlSi_{12}$ B2 As Built															
				Dry mass (g)				**Wet Mass (g)**							
Specimen	**Sample Label**	**T_{water} (°C)**	**ρ_{water} (g/mL)**	**1**	**2**	**3**	**AVG**	**1**	**2**	**3**	**AVG**	**ρ (g/mL)**			
1	**b21**	22.4	0.998	10.850	10.850	10.850	10.850	6.725	6.726	6.727	6.726	2.625		**ρ_{AVG}**	2.63
2	**b22**	22.4	0.998	10.884	10.884	10.884	10.884	6.748	6.749	6.749	6.749	2.626			
3	**b23**	22.4	0.998	10.957	10.957	10.957	10.957	6.819	6.821	6.820	6.820	2.643			
$AlSi_{12}$ B3 As Built															
				Dry mass (g)				**Wet Mass (g)**							
Specimen	**mple Lab**	**water (°C**	**ater (g/m**	**1**	**2**	**3**	**AVG**	**1**	**2**	**3**	**AVG**	**ρ (g/mL)**			
4	**b31**	22.4	0.998	10.799	10.799	10.799	10.799	6.673	6.674	6.674	6.674	2.612		**ρ_{AVG}**	2.61
5	**b32**	22.4	0.998	10.833	10.833	10.833	10.833	6.697	6.699	6.699	6.698	2.614			
6	**b33**	22.4	0.998	10.801	10.801	10.801	10.801	6.675	6.676	6.677	6.676	2.612			
$AlSi_{12}$ B3 Support															
				Dry mass (g)				**Wet Mass (g)**							
Specimen	**mple Lab**	**water (°C**	**ater (g/m**	**1**	**2**	**3**	**AVG**	**1**	**2**	**3**	**AVG**	**ρ (g/mL)**			
7	**b3s1**	22.4	0.998	11.441	11.441	11.441	11.441	7.148	7.149	7.149	7.149	2.659		**ρ_{AVG}**	2.66
8	**b3s2**	22.4	0.998	11.490	11.490	11.490	11.490	7.178	7.180	7.179	7.179	2.659			
9	**b3s3**	22.4	0.998	11.442	11.442	11.442	11.442	7.148	7.150	7.150	7.149	2.659			

Surface Roughness - The surface roughness of a section from the interior and exterior of an AM-built part was measured using a Keyence laser profilometer. The average of 4 scans (2mm x 2mm) showed that the interior surface of an AM-built part was smoother than the exterior surface of an AM-built part.

Hardness Testing **-** Vickers microhardness (major load of 500 grams) traverses were performed on a representative as-built piece of material. The average hardness of the part was 117.9 +/- 16.6 HV (average of 171 readings).

Heat Treatment of AM Build – Although post processing heat treatment of this powder was not recommended by the manufacturer, a heat treatment was performed on a few specimens, with parameters found in open literature for this alloy (500°C for 2 hours). This treatment differed greatly from the T6 treatment recommended for a cast 356 aluminum component (shown in Table 10). Research after the fact showed that literature exists that provides recommended heat treatment schedules for strengthening aluminum powder AM builds. For instance, one reference for heat treatment of AlSi10Mg alloy (similar to the one used in this study) lists a schedule of solid solution at 535°C (995°F) and artificial aging at 158°C (316°F) [24], which are almost the same as listed in Table 12 for cast A355 and A356 aluminum alloy. Future work could focus on trying this alternative heat treatment on AlSi12 AM builds to determine if mechanical properties could be optimized.

Tensile Testing - Tensile tests were conducted on specimens built with the actual parts using both the build and support parameters (shown previously in Table 12). Testing was accomplished in accordance with ASTM E8M-09 and with dynamic image correlation (DIC) VIC software to measure elongation. The specimens were sub-sized flat dogbones, and were tested at 1.25 mm/min in tension. The results showed that it appeared that the specimen representing the support structure parameters had the best combination of strength and elongation, slightly better than the specimens that had used the build parameters. Heat treatment degraded the mechanical properties, suggesting that an alternate heat treatment needs to be studied for improved post-treatment properties.

Metallography - Samples utilizing the as-built parameters, the support structure parameters, and heat-treated were subjected to metallographic inspection. The samples were ground and polished, and etched with a modified Murakami reagent. Figures 6, 7, and 8 are scanning electron micrographs of the support structure parameters representative material at low (figure 6) and high (figure 7) magnifications. In figure 6, note the “weld bead-type” patterns representing the laser melted regions that had solidified, common with DMLS processes. Also note the porosity (entrapped gas bubbles) within the sample. Figure 7 shows the dendrites (feathery structure) indicative of the aluminum cooling and solidifying from a molten state. Figure 8 shows a cavity-like defect that appears to be located along a witness line within the structure of the sample.

After heat treatment, the dendritic structure was no longer evidenced, nor was the weld bead-type structure (see low magnification example in Figure 9). As this figure shows, heat treatment had formed many precipitates, and what appears to be increased porosity. This porosity could be artifacts caused by pullouts of the precipitates during metallographic preparation and were not studied further.

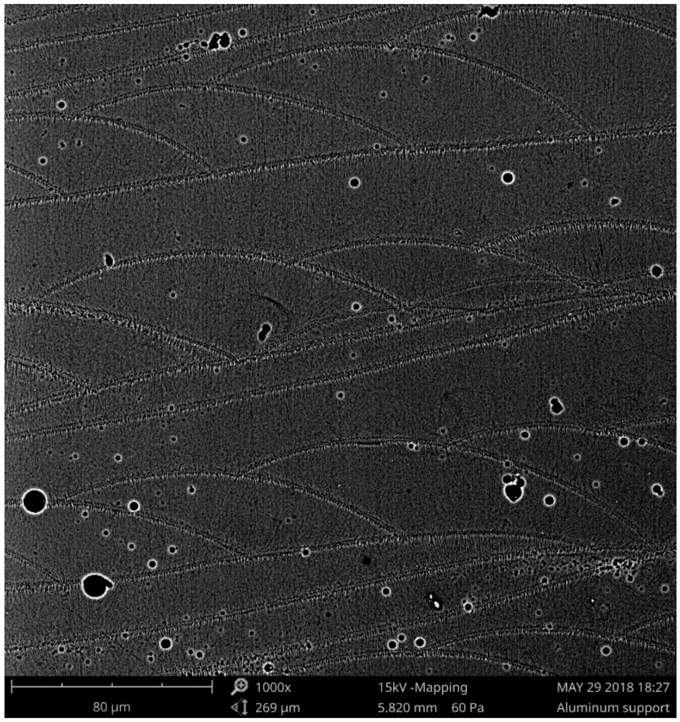

Figure 6 Scanning electron micrograph showing the microstructure of the DMLS specimen using support-structure parameters (representative). Etchant: modified Murakami's etch.

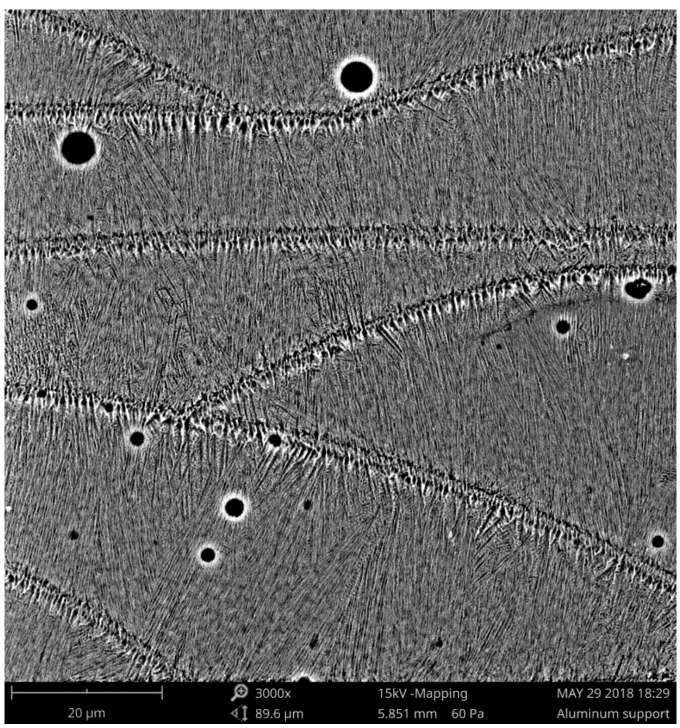

Figure 7 Higher magnification of the sample shown in Figure 6 – note dendrites (feathery structure) representing solidification of molten aluminum. Etchant: modified Murakami's etch.

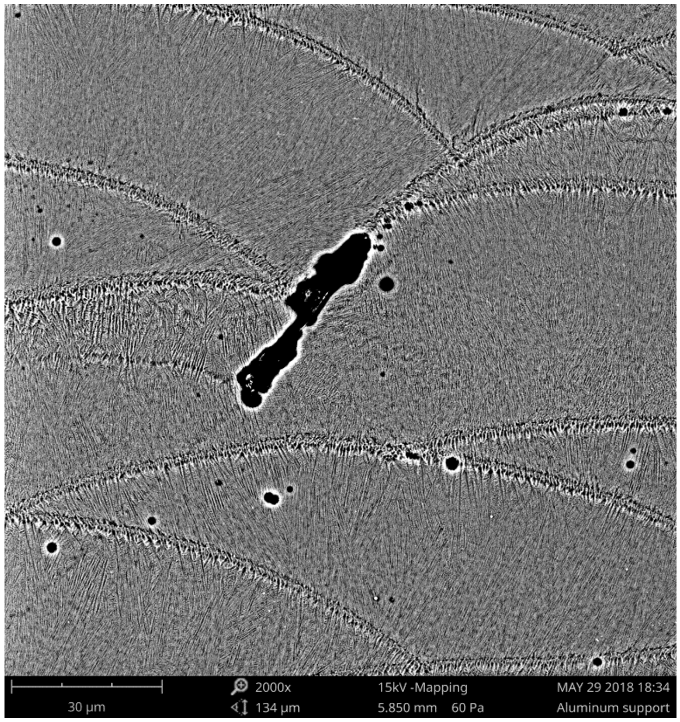

Figure 8 A cavity-like defect located on what appears to be a witness line within the structure of the sample. Etchant: modified Murakami's etch.

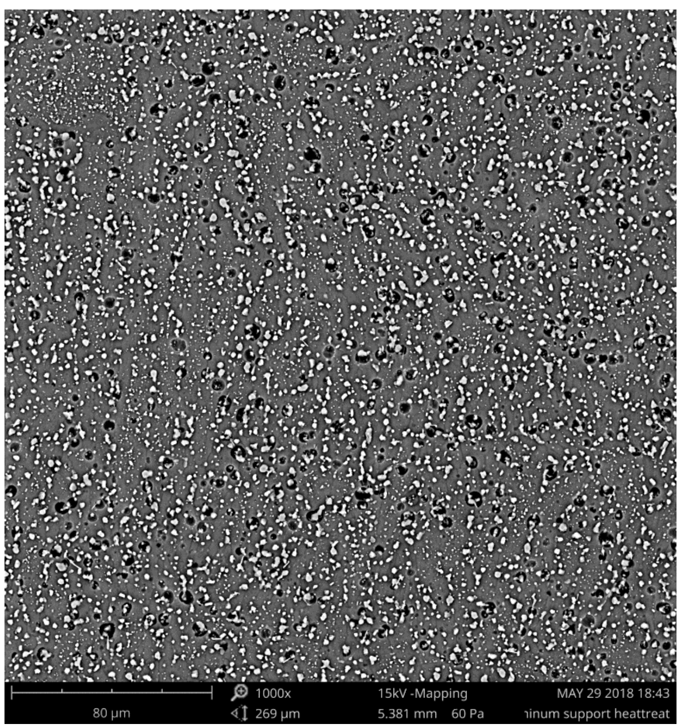

Figure 9 Structure of the sample representing the AM support structure parameters after heat treatment. Note the formation of precipitates, and the lack of any evidence of the dendrites and weld bead-type features noted prior to heat treatment. Etchant: modified Murakami's etch.

Business Case / Cost Comparison

Based on the amount of work needed to process indigenous sand for use as a viable 3D-printed mold material at the point-of-need (and the choice herein of desert versus beach sand), a true cost comparison could not be made. Listed below, however, are the costs needed to build these parts using metal additive manufacturing in a lab setting:

- 4 hours pre-processing time (human time)
- 100 hours print time (machine time)
- 4-6 hours post processing time (mostly machine time)
- Power requirement: 400 V / 15 KVA / 3 phase
- Powder cost: ~$800 per part (a lot of this powder is excess and can be reused though so actual cost would decrease with increased quantity)
- Al build platform cost: $280 (these are reusable)

In addition, thermal post-processing may be necessary, which would increase the total cost of AM production.

Lessons Learned

- 3D-Printing with Desert Sand:
  - Effect of clay contamination within the desert sand…will this affect the mold build?
  - Use of ultrafine desert sand clearly the most difficult path; beach sand with less fines may have been easier to work with.
  - Desert sand will require a modification to the 3D-printing process.
  - Developed a new screening process to remove large aggregates and most fines.
  - Alternative binder material was found to show improvement in bond strength, but further enhancement is needed.
  - Dry acid catalyst was found to work well with non-optimal, sub-par materials, and provided ability to print with fine materials.
  - Fast tooling was shown to be possible with sand printed molds.
- AM Builds
  - Ensure digital file is accurate prior to printing.
  - Choose an appropriate heat treatment that optimizes final properties.
  - As shown through CT, uninterrupted builds are key to better properties.

Future Work

Indigenous sand screening - The screening of the sand to the appropriate/acceptable particle size distribution turned out to be a monumental task. Dr. Peter Lucon [25], Assistant Professor of Mechanical Engineering, Department of Mechanical Engineering, Montana Tech University (and holder of many patents in the area of resonant acoustic mixing when employed by Resodyn Corp.) believes the RAM technology may offer a solution. Dr. Lucon mentioned that the benchtop RAM would be able to sieve 100 grams of sand in less than a minute. Research would be needed to upgrade the RAM system into a continuous-feed system to provide sieving capability to the size distribution needed and to determine if it can not only screen out the large aggregate but also the fines.

Improved indigenous sand binder - The current commercial resin is not strong enough to work with the fine particles of desert sand that cannot be removed. The binder used was well above the range specified by the supplier (and outside the range that is currently able to be deposited by a 3D printer). Trying to maintain a recipe that was usable in a 3D printer was the main constraint, and anything higher than what was tried wouldn't be feasible. As mentioned, foundry binder strength development is generally complete after 24 hours, and will not increase after that point. The inorganic resin used herein showed promise in increasing the strength of the mold 3D-printed from indigenous sand. This is most likely due to it utilizing the fine particles for bonding. Further work in this area would be beneficial, for successful, this would represent a major step in using indigenous materials for additive manufacturing.

Improved AM build thermal post-treatment - As listed herein, the heat treatment utilized on the AM-built samples actually lowered the strength of the material. Work could be performed in this area in an attempt to find an optimal thermal post treatment (if any) for maximized mechanical properties of AM builds using the AlSi12 alloy powder.

Acknowledgements
The authors wish to thank Dr. Rik Riman (Rutgers University) for his guidance on (and sample of) low-temperature solidified ceramic binders, and Tony Delgado and Eric Kirchner (DLA) for their funding of this project, and their continued inputs along the way.

References
[1] "Digital Metal: AM for Casting Metal Parts in Architecture", M. Meibodi, TCT Magazine, Volume 4, Issue 4.
[2] "Aerospace Project Pairs 3D Printing with Investment Casting", S. Hendrixson, Additive Manufacturing, November 2017, p. 64.
[3] "http://earth.sustainablesources.com, referenced 12/8/11.
[4] "Force Projection Research and Development: The Key Enabler for Army Transformation", Col Genaro J. Dellarocco, 10 April 2001.
[5] "US Army Outlines Push to Save Resources, Lives", Defense News, 11/19/13.
[6] "Shrinking the Logistics Tail in the Combat Zone", Col Larry W. Jameson, 9 April 2002.
[7] "Logistics Transformation – Reducing the Logistics Footprint", LTC Darrell S. Ransom, 5 April 2002.
[8] "Sand Printing Expands Metal Possibilities, Too", Additive Manufacturing, November 2016, p. 37.
[9] "4063 Additive Manufacturing for Metal casting (AM4MC)", presentation by R. Lonardo and N. Pramanik for America Makes, referenced on 7 March 2017.
[10] "The Effects of 3D Printed Molds on Metal Castings", D. Snelling, et. al., Proceedings of the Solid Freeform Fabrication Symposium (2013), pp. 827-845.
[11] "Additive Manufacturing of Molds for Sand Casting", N. Hawaldar and J. Zhang, Poster at the Powdermet 2017 conference, Las Vegas, NV, 14 June 2017.
[12] "Quantifying the Role of Part Design Complexity in Using 3D Sand Printing for Molds and Cores", E. Almaghariz et. al., International Journal of Metalcasting, Volume 10, Issue 3, 2016.

[13] “Paradigm Shift”, B. Connor, Defense AT&L Journal, Special Issue – Additive Manufacturing (3D Printing), November-December 2016.
[14] “AM Answers its Casting Call”, B. Donaldson, Additive Manufacturing, November 2017.
[15] “Comparative Study of 3D Printing Technologies for Rapid Casting of Aluminum Alloy”, S. Singh Gill et. al., Journal of Materials and Manufacturing Processes, 24, pp. 1405-1411, 2009.
[16] “Guide to Casting and Molding Processes”, 2015 Metal Casting Design and Purchasing Journal.
[17] “Reclamation and reusability studies on CO2 sodium silicate bonded sands for ferrous foundries”, SM Nazirudeen, 13_Chapter 4, 1999.
[18] Foseco Ferrous Foundryman’s Handbook, edited by John Brown, Butterworth-Heinemann, 2000.
[19] “Critical Characteristics Affecting the Surface Finish of Castings”, N. Bryant and J. Thiel, AFS Transactions, Paper 17-094 v125, 2017.
[20] “Aluminum Heat Treatment Revisited: Common Concerns and How to Resolve Them”, D. Herring, Industrial Heating, February, 2018, p. 18.
[21] ASTM B917, “Standard Practice for Heat Treatment of Aluminum-Alloy Castings from All Processes”, 2012, ASTM, Conshohocken, PA.
[22] Luvak Inc. Analytical Report No. 0-82641, 10/5/17, provided by Andrew Burke, Quality Manager.
[23] “Influence of Powder Characteristics on Processability of AlSi12 Alloy Fabricated by Selective Laser Melting”, R. Baitimerov, et. al., MDPI, Materials, 5/7/18.
[24] “Using Two-Stage T6 Heat Treatment to Tailor the Mechanical Properties of 3D Printed Aluminum AlSi10Mg Alloy, S. Saunders, 3Dprint.com, 8/20/18.
[25] Personal correspondence with Dr. Peter Lucon, Assistant Professor of Mechanical Engineering, Department of Mechanical Engineering, Montana Tech University on 2/7/18 and follow up electronic correspondence on 2/20/18.